Cardiff Economics Working Papers



Working Paper No. E2025/19

Adaptive-Lasso MGARCH for the Volatility Spillover of Transition Finance

Yongdeng Xu, Juyi Lyu and Khelifa Mazouz

September 2025

ISSN 1749-6010

Cardiff Business School
Cardiff University
Colum Drive
Cardiff CF10 3EU
United Kingdom
t: +44 (0)29 2087 4000
f: +44 (0)29 2087 4419
business.cardiff.ac.uk

This working paper is produced for discussion purpose. These working papers are expected to be published in due course, in revised form.
Cardiff Economics Working Papers are available online from:
http://econpapers.repec.org/paper/cdfwpaper/ and
https://carbsecon.com/wp/index_abstracts.html
Enquiries: EconWP@cardiff.ac.uk

Adaptive-Lasso MGARCH for the Volatility Spillover of Transition Finance

Yongdeng Xu [*] Juyi Lyu [†] Khelifa Mazouz [‡]

September 22, 2025

Abstract

Most transition-finance assets (green bonds, EU emission allowances, clean-energy equities) have only a few years of daily data and virtually no intraday history, rendering standard spillover tools either infeasible (high-dimensional MGARCH) or inapplicable (realized-variance VARs). We develop an Adaptive-Lasso MGARCH (AL-MGARCH) estimator that applies an L_1 penalty with adaptive weights to shrink negligible cross-effects to zero, reducing the active parameter set from $O(N^2)$ to $O(N)$ while retaining oracle-selection properties. We also generalise Diebold–Yilmaz–style connectedness to daily returns, enabling single-step monitoring of transition-risk networks when intraday data are unavailable. Using eight daily series (2018–2025), we document a bond-centred volatility regime before 2022 and a natural-gas- and coal-centred regime after the Russia–Ukraine shock, reconciling mixed evidence on whether green assets hedge or amplify systemic risk.

Keywords: adaptive Lasso; MGARCH; volatility spillovers; green bonds; clean-energy equities; carbon allowances; transition finance

JEL classification: C58; G15; Q40; Q54

[*]Cardiff University, Cardiff, UK; Email: xuy16@cardiff.ac.uk
[†]Loughborough University, UK; Email: julielyu2014@gmail.com
[‡]Corresponding Author, Cardiff University, Cardiff, UK; Email: mazouzk@cardiff.ac.uk

1 Introduction

Volatility has become the dominant language of financial risk in the energy-transition era. Coal prices collapsed by 60% between 2012 and 2016, only to triple during the 2022 supply crunch; EU emission-allowance (EUA) futures oscillated between EUR 5 and EUR 100 over the past decade; and labelled green bonds, virtually non-existent before 2010, now display dynamics that conventional fixed-income benchmarks cannot explain. Understanding how shocks propagate across this mixed universe of green and conventional assets is therefore central to not only portfolio resilience and hedging design, but also the macro-prudential foundations of climate policy and the credibility of the low-carbon transition. Empirical answers, however, remain contradictory.

Most transition-finance assets offer only a few years of daily prices and virtually no reliable intraday history. A typical researcher therefore faces a panel of 1600–1800 observations but would like to track ten or more markets at once. The three main econometric approaches used in the spillover literature to address the "short-T, large-N" problem each encounter limitations, albeit for different reasons, when applied to transition-finance assets with sparse data.

First, *realized-variance VARs* underpin the Diebold–Yilmaz connectedness index and its HAR-VAR or TVP-VAR extensions (Diebold and Yilmaz, 2012, 2014; Corsi, 2009; Antonakakis et al., 2020; Gabauer and Gupta, 2018). These models scale almost costlessly with the cross-section because the variance–covariance matrix is obtained from ordinary least squares, but they need high-frequency returns to construct daily realized volatilities. Such data simply do not exist for labelled green bonds, EU-ETS allowances or technology-pure solar and wind indices that began trading only in the mid-2010s. Second, *multivariate GARCH* specifications work directly with daily returns and embed spillovers in the conditional-covariance matrix (Engle and Kroner, 1995; Bauwens et al., 2006). Extensions such as the vector MEM of Xu et al. (2018) and the asymmet-

ric MGARCH of Xu et al. (2024) show how macro-shocks and illiquidity feed through volatility networks, but the price is dimensional: a MGARCH(1,1) entails $O(N^2)$ coefficients. Estimation becomes numerically unstable once N is large - often already for $N > 4$ (Bauwens et al., 2006))- well below the number of markets required to study the full green–conventional universe. Third, *two-step GARCH–VAR hybrids* estimate a separate univariate GARCH for each series and then feed the fitted volatilities into a VAR (Hamao et al., 1990; Koutmos, 1999; Ewing and Payne, 2003; Sánchez García and Cruz Rambaud, 2023; Vo, 2023; Díaz and Livingston, 2025). While computationally convenient, the approach inherits bias and inefficiency because first-stage volatilities are noisy estimates, not observed variables; any error in stage one contaminates the VAR coefficients and, by extension, the connectedness statistics.

These methodological limitations hinder reliable inference in the interaction of fossil-fuel, carbon, and green-asset markets in the transition era. To close this gap, we propose an Adaptive-Lasso MGARCH (AL-MGARCH) estimator, which is a single-step framework that preserves the daily-data feasibility of MGARCH while taming dimensionality through data-driven sparsity. The approach adds an L_1 penalty with data-driven adaptive weights to the quasi-likelihood. Coefficients associated with weak cross-market effects shrink exactly to zero, whereas economically important links remain untouched. Because the weighting follows the adaptive-Lasso principle of Zou (2006), the estimator retains oracle variable-selection consistency while reducing the active parameter count from $O(N^2)$ to $O(N)$.

An overlooked advantage of the AL-MGARCH representation is that it allows the Diebold–Yilmaz spillover index to be generalised to daily-return data. By recasting the MGARCH in vector-MEM form, we obtain closed-form multi-step forecasts, from which impulse responses and directional connectedness measures follow without the need for realized volatilities. The approach preserves the economic intuition of the original index, which reflects variance shares attributable to cross-market shocks, while freeing the

researcher from the intraday data requirement that has limited application to transition-finance assets.

We apply the AL-MGARCH to an eight-asset panel comprising a labelled green-bond index, the USD-hedged Bloomberg Global Aggregate, Brent crude, a global LNG benchmark, ICE Rotterdam coal futures, EUA futures, the MSCI All-Country World equity index and the MSCI ESG Leaders sleeve. The full-sample results (2018–2025) indicate a bond-centred volatility regime, in which both conventional and green bonds are net transmitters, while natural gas, crude oil and coal mainly absorb shocks.

Replacing the aggregated SCI ESG sleeve with technology-specific Solactive Solar and Solactive Wind indices reveals that solar equities, not the diversified clean-energy basket, carry the largest outbound spillovers. This provides evidence that technology-targeted subsidies can create new high-beta channels. A subsample estimated from 24 February 2022, when Russia's invasion of Ukraine re-ordered energy priorities, shows a regime switch in which natural gas and coal contracts become the dominant transmitters, with bond markets absorbing rather than exporting volatility. These findings reconcile earlier contradictions in the literature on whether green assets hedge or amplify systemic risk, which depends critically on the macro regime and the level of technological granularity at which green equities are modelled.

The paper makes three contributions. First, it provides the first single-step estimation and selection procedure for high-dimensional MGARCH models based solely on daily data. This bridges the gap between tractability and dimensionality that has hampered spillover research in green finance. Second, it extends the Diebold–Yilmaz connectedness framework to settings where realized volatilities are unavailable, thus unlocking analysis for the full range of transition-finance assets. Finally, it delivers new evidence on how volatility migrates between fossil-fuel contracts, carbon prices, labelled bonds and technology-specific equities, demonstrating that transition risk is regime-dependent and technology-sensitive rather than uniformly hedging or amplifying.

The remainder of the article proceeds as follows. Section 2 describes the empirical methodology, covering the the Adaptive Lasso MGARCH estimator and the construction of the spillover index. Section 3 introduces the data. Section 4 presents empirical results. Finally, Section 5 concludes.

2 Methodology

2.1 Adaptive-Lasso MGARCH model

We model multivariate volatility of daily returns using a MGARCH(1,1) framework with constant conditional correlations (CCC), with particular interest in estimating volatility spillovers between assets. Let $\mathbf{r}_t$ denote an $N \times 1$ vector of demeaned asset returns following a MGARCH(1,1) specification.

Following Conrad and Karanasos (2010), returns are modeled as:

$$\mathbf{r}_t = \boldsymbol{\varepsilon}_t, \qquad \boldsymbol{\varepsilon}_t = \mathbf{D}_t \mathbf{e}_t, \tag{1}$$

$$\mathbf{h}_t = \boldsymbol{\omega} + \mathbf{A}\boldsymbol{\varepsilon}_{t-1}^2 + \mathbf{B}\mathbf{h}_{t-1}, \tag{2}$$

where $\mathbf{D}_t = \text{diag}(\mathbf{h}_t^{1/2})$ is a diagonal matrix of conditional standard deviations, and $\mathbf{e}_t | I_{t-1} \sim N(\mathbf{0}, \mathbf{P})$. Consequently, $\mathbb{E}(\boldsymbol{\varepsilon}_t | I_{t-1}) = \mathbf{0}$ and $\mathbb{E}(\boldsymbol{\varepsilon}_t \boldsymbol{\varepsilon}_t' | I_{t-1}) = \mathbf{H}_t = \mathbf{D}_t \mathbf{P} \mathbf{D}_t$, where I_t denotes the information set available up to time t. The framework can be extended to include higher-order lags or asymmetric terms without fundamental changes to the estimation approach.

When $\boldsymbol{\omega} > 0$ and $\mathbf{A}$, $\mathbf{B}$ are unrestricted $N \times N$ matrices as in Conrad and Karanasos (2010), the variance equation contains $2N^2 + N$ parameters. This parameter proliferation presents a fundamental challenge in MGARCH modeling: maintaining flexibility while preventing dimensional explosion as N grows (see Bauwens et al. (2006)). Richly parameterized models with $O(N^2)$ parameters become infeasible for moderate to large

N, forcing researchers toward restricted specifications like scalar or diagonal models with only $O(1)$ or $O(N)$ parameters. While these parsimonious alternatives mitigate estimation challenges, they sacrifice the very flexibility needed to capture complex volatility spillover patterns.

To address this trade-off, we implement an Adaptive Lasso approach that applies L_1 penalization to cross-asset coefficients with data-driven weights. This method aggressively shrinks minor cross-effects toward zero while preserving significant spillovers. The Adaptive Lasso improves upon standard Lasso by downweighting penalties on larger coefficients, enhancing variable selection consistency (Zou, 2006). Defining the scaled negative log-likelihood as:

$$\bar{\ell}_T(\boldsymbol{\theta}) = -\frac{1}{T}\sum_{t=1}^{T} \ln f(\boldsymbol{\varepsilon}_t \mid \boldsymbol{\theta})$$

denote the scaled negative log–likelihood, where $\boldsymbol{\theta}$ includes the parameters in the conditional variance equations (w, A, B). The penalized estimator solves

$$\widehat{\boldsymbol{\theta}}(\lambda) = \arg\min_{\boldsymbol{\theta}} \left\{ \bar{\ell}_T(\boldsymbol{\theta}) + \lambda \sum_{j=1}^{d} w_j \, |\boldsymbol{\theta_j}| \right\}, \tag{3}$$

where d is the number of penalized coefficients, λ is a tuning parameter controlling the overall penalty strength, and w_j are data-driven weights (typically $w_j = 1/|\tilde{\theta}_j|$), where $\tilde{\boldsymbol{\theta}}$ is a preliminary unpenalized QML estimator). The L_1 penalty induces sparsity: as Zou (2006) note, L_1 regularization "shrinks off-diagonal elements toward zero, typically resulting in many estimates being identically zero." Thus, minor spillover parameters are eliminated, leaving only economically significant volatility links.

The tuning parameter λ governs the trade-off between model fit and sparsity. We select it using data-driven methods such as cross-validation or information criteria applied to a hold-out sample. The procedure involves splitting the data into training and

validation sets, estimating the model for candidate λ values on the training data, and evaluating out-of-sample performance on the validation set. The optimal λ minimizes this validation loss, automatically determining the appropriate degree of regularization: larger values yield sparser models with fewer nonzero coefficients, while smaller values approach the unpenalized MGARCH solution. Final estimation proceeds by maximizing the penalized likelihood with the selected λ, typically through iterative optimization algorithms. This L_1 penalization effectively reduces parameter dimensionality from $O(N^2)$ to $O(N)$ (see, e.g., Cattivelli and Gallo (2019)). Appendix A details the procedure for selecting the tuning parameter $\hat{\lambda}$ and the full estimation algorithm.

The Adaptive-Lasso MGARCH combines the practical advantages of daily GARCH modeling with rigorous dimensionality control through regularization. By automatically eliminating negligible cross-asset effects, it delivers a scalable, single-step estimator that identifies economically significant volatility transmission channels—particularly valuable in settings like energy-finance markets where intraday data are limited but cross-asset monitoring remains crucial.

2.2 Spillover Analysis

Having estimated the Adaptive-Lasso MGARCH model, we now analyze volatility spillovers across markets. Following the methodologies of Engle et al. (2012) and Xu et al. (2018), we develop quantitative measures of volatility spillover effects based on shock propagation analysis.

MGARCH model can be expressed as a multiplicative error form:

$$\begin{aligned} \boldsymbol{\varepsilon}_t &= \sqrt{\mathbf{h}_t} \odot \boldsymbol{e}_t, \quad \boldsymbol{e}_t \sim \mathrm{N}(\mathbf{0}, \boldsymbol{P}), \\ \mathbf{h}_t &= \boldsymbol{\omega} + \mathbf{A}\boldsymbol{\varepsilon}_{t-1}^2 + \mathbf{B}\mathbf{h}_{t-1}. \end{aligned} \tag{4}$$

where $\odot$ denotes the Hadamard (element-wise) product, and $\boldsymbol{\varepsilon}_t = \mathbf{r}_t$ represents the

demeaned returns. The innovation vector $\boldsymbol{e}_t$ has zero mean and variance-covariance matrix $\boldsymbol{P}$.

Next, we derive a multiple-step ahead forecasting $\mathbf{h}_{t+\tau}$ (where $\tau > 0$). The forecast is computed at date t, but since it is not known, it needs to be substituted with its corresponding conditional expectation $\mathbf{h}_{t+\tau|t}$. Hence:

$$\mathbf{h}_{t+1|t} = \boldsymbol{\omega} + \mathbf{A}\boldsymbol{\varepsilon}_t^2 + \mathbf{B}\mathbf{h}_t, \tag{5}$$

and for any $\tau \geq 2$,

$$\mathbf{h}_{t+\tau|t} = \boldsymbol{\omega} + (\mathbf{A} + \mathbf{B})\mathbf{h}_{t+\tau-1} \tag{6}$$

which can be solved recursively for any horizon τ.

Next, we derive a spillover balance index and spillover asymmetry measure. Let us recall that the MEM in a system,

$$\mathbf{r}_t = \sqrt{\mathbf{h}_t} \odot \boldsymbol{e}_t, \quad \boldsymbol{e}_t \sim \mathrm{N}(\mathbf{0}, \boldsymbol{P}). \tag{7}$$

The innovation vector $\boldsymbol{e}_t$ has a mean vector $\mathbf{0}$ and general variance-covariance matrix $\boldsymbol{P}$. We can interpret $\mathbf{h}_{t+\tau} = E(\mathbf{r}_{t+\tau}^2 | I_t, \boldsymbol{e}_t = \mathbf{0}) =$, that is, the expectation of $\mathbf{r}_{t+\tau}^2$ conditional on $\boldsymbol{e}_t$ being equal to the zero vector: this is the basis for the dynamic forecast obtained before. Let us now derive a different dynamic solution, $\mathbf{h}_{t+\tau}^{(i)} = E(\mathbf{r}_{t+\tau}^2 | I_t, \boldsymbol{e}_t = \mathbf{0} + \mathbf{s}^{(i)})$, for a generic ith element $\mathbf{s}^{(i)}$, where $i = 1, 2, ..., N$. The ith element equal to the unconditional standard deviation of $e_{i,t}$ and the other terms $j \neq i$ equal to the linear projection $E(e_{j,t}|e_{i,t})$. The element-by-element division ($\oslash$) of the two vectors,

$$\rho_{t,\tau}^{(i)} = \mathbf{h}_{t+\tau}^{(i)} \oslash \mathbf{h}_{t+\tau} - 1. \tag{8}$$

Given the multiplicative nature of the model, $\rho_{t,\tau}^{(i)}$ gives us the set of responses (relative changes) in the forecast profile starting at time t for a horizon τ brought about a

1 standard deviation shock in the ith market. The cumulated impact of the shock from market i to market j is:

$$\Phi_t^{j,i} = \sum_{\tau=1}^{K} \rho_{t,\tau}^{(i)}. \tag{9}$$

The total spillover effect (TSI) as:

$$TSI = \sum_{i \neq j} \sum_{t=1}^{T} \Phi_t^{j,i} \tag{10}$$

which measures the overall contribution of volatility spillover shocks across markets.

This is also a way to assess the total change induced by the shock of different markets. Following Xu et al. (2018), we express the spillover balance as the ratio of the average responses "to" to the average response "from" (excluding one's own):

$$Balance_i = \frac{\sum_{j \neq i} \sum_{t=1}^{T} \Phi_t^{j,i}}{\sum_{j \neq i} \sum_{t=1}^{T} \Phi_t^{i,j}}. \tag{11}$$

A balance bigger than unity signals that the market is a net creator of volatility spillover, while a value less than unity identifies it as a net receiver.

3 Data

Our empirical universe comprises eight daily time series designed to capture the principal channels through which climate-transition news, commodity shocks and global risk appetite transmit volatility. These include two bond indices (green and conventional), three energy/commodity prices (crude oil, coal, and natural gas), carbon permits, and two equity benchmarks (conventional and ESG). We focus on eight daily series to ensure each market has a clear economic role while keeping the parameter count manageable relative to the 1,700 observations (January 2018 - June 2025). All prices are New-York closes converted to USD; log-returns are multiplied by 100 to express percentage units.

Green bonds are proxied by the Solactive Green Bond Index, a USD total-return measure of labelled issues dedicated to climate projects. Data (available since 2012, via LSEG Datastream) are widely used in the literature (e.g.,Reboredo, 2018; Saeed et al., 2021; Hassan et al., 2022), with evidence of distinct dynamics relative to conventional bonds (Reboredo et al., 2020; Mensi et al., 2024).

Conventional bonds are represented by the Bloomberg Global Aggregate Bond Index (USD-hedged), a broad benchmark of fixed-rate sovereign and corporate debt. The USD hedge version eliminates currency noises and isolates bond-market dynamics. Data are available from 2016 via Bloomberg and have been widely used (e.g., Arnold et al., 2024; Wang and Urga, 2025; Ito and Yoshiba, 2025)

Oil is proxied by ICE Brent front-month futures, the global crude benchmark reflecting transport and industrial demand. Daily data (since 1988, LSEG Datastream) are widely used in volatility studies (e.g., Mensi et al., 2021; Coskun and Taspinar, 2022; Wei et al., 2023; Fields and Lindequist, 2024; Ren et al., 2024).

Coal is measured by ICE Rotterdam (API2) futures, the global benchmark for thermal coal delivered to Europe. Daily data are available from 2010 (LSEG Datastream) and commonly used in energy studies (Coskun and Taspinar, 2022; Fields and Lindequist, 2024; Liu et al., 2025; Zeng et al., 2025).

Natural gas is proxied by the S&P GSCI 3-Month Forward Natural Gas Index (ER), based on Henry Hub futures. Its role as marginal fuel in power generation made it a key transmitter of volatility during the 2022–2024 energy crisis. Daily data are available from 1995 (LSEG Datastream), with applications in Liu (2022), Gurrib et al. (2022), Chen et al. (2023), and Leone et al. (2025).

Carbon markets are captured by EU Emissions Allowances (EUAs), the tradable permits of the EU-ETS. Prices signal the marginal cost of emitting one tonne of CO_2. Daily data are available from 2005 (LSEG Datastream) and widely used as standard carbon indicators (e.g., Zhang et al., 2022; Bouri et al., 2023; and Ren et al., 2024).

Global equities are represented by the MSCI ACWI (USD price), covering developed and emerging markets. Available since 1988 (LSEG Datastream), it is a standard gauge of risk appetite (Hachicha et al., 2022; Estrada, 2023; Scherer and Scherer, 2025; Kacperczyk et al., 2025). Studies show equities play a central role in volatility transmission (Kang et al., 2019; Xu et al., 2024).

Green equities are proxied by the MSCI Global Environment Index, composed of firms deriving at least half of revenues from environmentally beneficial activities. Daily data (since 2010, LSEG Datastream) are widely used as a green equity benchmark (e.g., Chatziantoniou et al., 2022; Tiwari et al., 2023; Lucey and Ren, 2023).

For robustness, we also use the Solactive Global Solar Energy Index (since 2018) and the Solactive Global Wind Energy Index (since 2017), both available from LSEG Datastream and focusing on firms directly engaged in clean energy. These indices are standard ESG equity benchmarks (Tiwari et al., 2022; Wang and Chang, 2023; Tiwari et al., 2023).

The data cover the period from 07/11/2018 to 19/02/2025, with a sample size of T=1509. This is the longest period during which all the assets mentioned above are traded and have available data. A sample size of T=1509 is sufficiently large to conduct our AL-MGARCH estimation with 128 parameters. The descriptive statistics for the prices and returns of these variables are summarised in Table 1, and their time series evolution is depicted in Figure 1.

Table 1 reveals three stylised facts. First, at the mean level, most series are mean-reverting around zero: EU Emission Allowances (EUA) are the only asset with a significant positive drift (0.333), while the green-equity index (ESG, 0.095) and the conventional equity index (STOCK, 0.086) show merely modest upticks. By contrast, natural gas records a small negative drift (GAS, -0.09), reflecting the prolonged weakness in global gas prices. The aggregate bond index (AGGB, -0.03) also trends slightly downward, consistent with the post-2017 "repricing of duration" triggered by rising long-term

Table 1 – Descriptive statistics of daily log–returns

	GBOND	**ESG**	**AGGB**	**BRENT**	**GAS**	**COAL**	**EUA**	**STOCK**
Min	-7.874	-24.843	-13.95	-70.50	-51.553	-135.294	-49.022	-25.192
Max	7.010	37.313	6.03	48.075	31.369	82.206	40.802	20.308
Mean	0.001	0.095	-0.03	0.036	-0.090	0.019	0.333	0.086
Std	1.193	4.764	0.90	6.613	7.116	8.046	7.464	2.643
Skew	-0.261	-0.001	-2.76	-1.344	-0.353	-2.606	-0.333	-1.059
Kurt	8.507	7.720	42.60	21.771	6.920	69.350	7.372	17.253
LB^2	312.148	251.603	10.501	435.717	398.796	59.899	213.785	1581.352

Note. GBOND: Solactive Green Bond Index; ESG: MSCI Global Environment index; AGGB: USD-hedged Bloomberg Global Aggregate; BRENT: ICE Brent Crude futures contract front-month; GAS: S&P GSCI 3-Month Forward Natural Gas Index (ER); COAL: ICE Rotterdam coal nearby; EUA: EU Emissions Allowances (EEX EUA); STOCK: MSCI All-Country World Index. LB^2 is the Ljung–Box statistic for squared returns (lag 20).

yields. Second, volatility varies widely across markets. The standard deviations of crude oil (6.613) and natural gas (7.116) are more than six times that of conventional bonds (AGGB, 0.9), with green bonds (GBOND, 1.193) sitting in between. This pattern aligns with the summary statistics reported in Reboredo et al. (2020) and Mensi et al. (2024), which show bond indices exhibit substantially lower volatility than energy commodities, underscoring their safe-haven role. Third, all distributions deviate from normality. Every asset shows negative skewness, reflecting frequent downside moves, and kurtosis is far above the Gaussian benchmark of three, reaching 42.6 for conventional bonds and 69.3 for coal. These results indicate fat tails and sharp peaks, characteristic of heavy-tailed behaviour. The Ljung–Box statistics for squared returns (lag 20) are highly significant in every column, confirming pronounced ARCH effects and justifying the use of a multivariate-GARCH specification in the subsequent analysis.

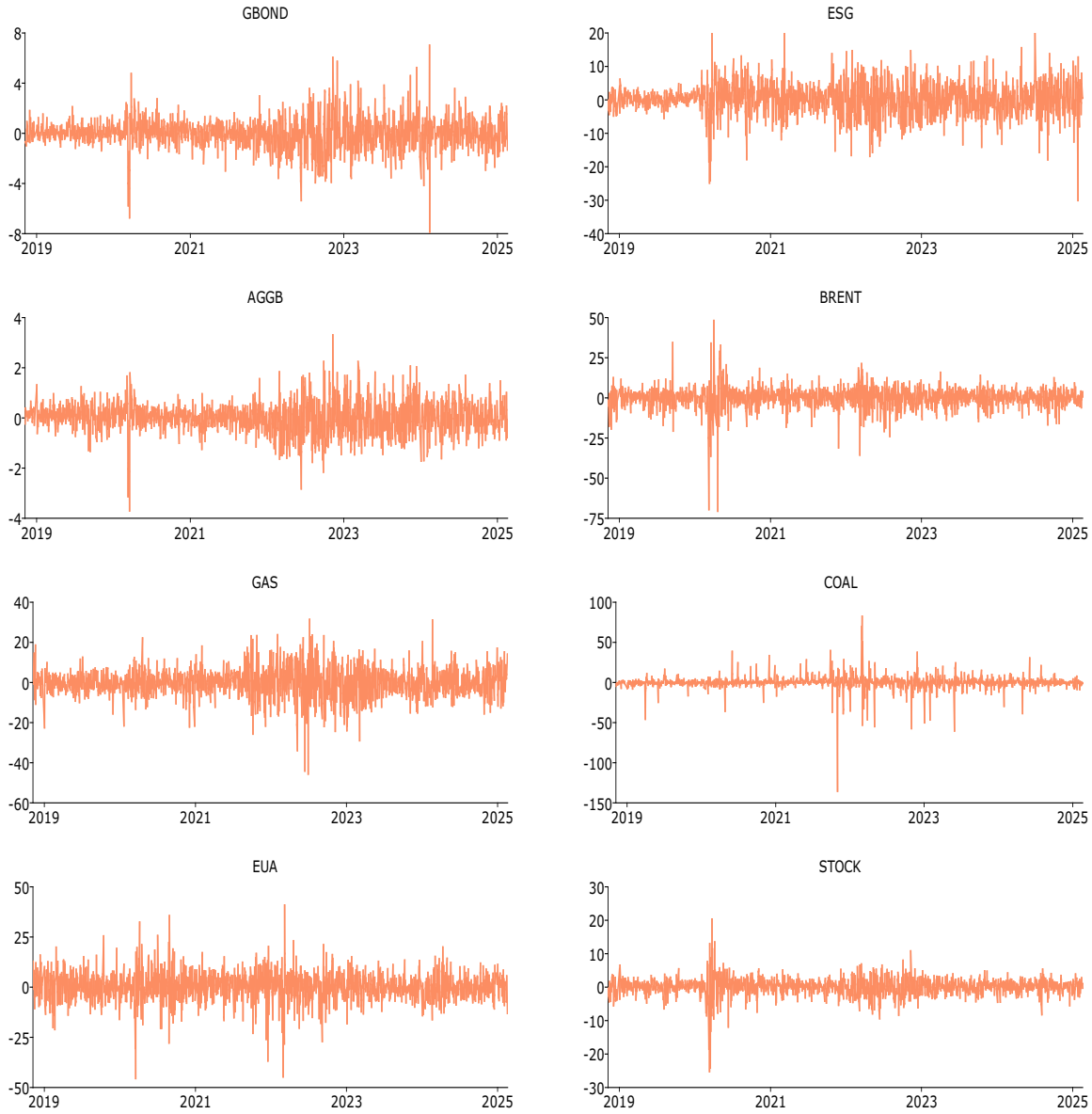


Figure 1 – Time evolution of returns for the eight assets

Figure 1 plots the daily log-returns of the eight benchmarks for 2018–2025. Several regime shifts stand out visually. First, the COVID-19 sell-off in March 2020 triggered a synchronised plunge across the aggregate bond index (AGGB), green bond index (GBOND), broad equity index (STOCK), ESG equity index (ESG), EU emission al-

lowance (EUA), and Brent crude (BRENT) indices, whereas GAS and COAL remained relatively muted - an early hint of the asymmetry between rate-driven assets and commodities later confirmed by the spillover matrix. Second, from mid-2021 the EU emission allowance (EUA) enters a persistent high-volatility phase that coincides with the Fit-for-55 package, while no comparable structural break is observed in the other assets, highlighting the policy-specific nature of carbon risk. Third, beginning in February 2022 the GAS and COAL series display unprecedented spikes that coincide with the Russia–Ukraine energy shock; later robustness checks show that in the post-war subsample, natural gas switches role and becomes a net transmitter of volatility. Finally, the Solar and Wind indices (when included) display higher-frequency swings after August 2022, consistent with the Inflation Reduction Act's revaluation of renewable-equity cash flows. Overall, the volatility spikes line up with the policy dates, validating the impulse-response analysis and the subsample split discussed in later sections.

4 Empirical Results

This section presents the main findings of our analysis, organised into five subsections. We begin with the results from the AL-MGARCH estimation, followed by the spillover analysis and the impulse response analysis. We then conduct robustness checks to assess the stability of the findings, and conclude with policy implications derived from the empirical evidence.

4.1 Results from the AL-MGARCH model

In the first subsection, we present the estimated results of the AL-MGARCH model. The estimation window is divided into two intervals of 1000 and 509 observations, respectively. The first interval is used to evaluate the optimal shrinkage parameters λ_T. The Adaptive Lasso estimates β_{λ_T} are then obtained using the full sample.

Table 2 – Adaptive-Lasso estimates of the coefficient matrices **A** and **B**

	GBOND	**ESG**	**AGGB**	**BRENT**	**GAS**	**COAL**	**EUA**	**STOCK**
				Matrix **A**				
GBOND	0.1084	0.0535	0.0202	0	0.0342	-0.0013	-0.0017	0
ESG	0.0218	0.1579	0	0.0125	0.0187	-0.0044	0.0086	-0.0015
AGGB	0.0099	0.0021	0.0979	0.0061	0.0520	0.0075	0.0030	0.0155
BRENT	-0.0050	0.0036	0.0761	0.1958	0.0079	0	0.0263	0.1011
GAS	0.0659	0	0.0418	0.0158	0.1512	0.0016	0.0019	0.0017
COAL	0.1081	-0.0051	-0.0300	0.0012	0.1198	0.0968	0.0061	-0.0230
EUA	0.0029	0.0070	0	0.0140	0.0092	0.0308	0.1218	0.0491
STOCK	0	0.0158	0.0127	0.0788	0	-0.0021	0.0259	0.1779
				Matrix **B**				
GBOND	0.7107	0.0021	0.0737	0.0060	0.0061	0.0049	-0.0245	-0.0030
ESG	0.0674	0.6092	0.0235	0.0073	0.0201	0.0098	-0.0018	0.0245
AGGB	0.0188	0	0.7931	0	-0.0074	0	-0.0035	-0.0273
BRENT	0.0062	0.0127	0.0213	0.2794	-0.0024	-0.0041	0.0270	0.0805
GAS	0.0607	0.0351	0.0527	0.0065	0.4544	0.0312	-0.0024	-0.0024
COAL	0.0162	0.0491	0.0290	0.0062	0.0432	0.4273	0.0565	-0.0062
EUA	-0.0082	0.0043	-0.0187	-0.0013	0.0050	0	0.5926	0.0187
STOCK	0.0125	0.0347	0	0.0267	-0.0015	0	0.0201	0.5458

Note: Elements set exactly to zero by the penalty appear as "0". Standard errors (or t-ratios) are available upon request.

Table 2 reports the estimated results. In both ARCH coefficient (Matrix A), and GARCH coefficient (Matrix B), elements set exactly to zero by the penalty appear as "0". Matrix A shows the "shock-propagation" (ARCH) effects in the short run. Several off-diagonals survive the penalty, with green-bond innovations transmitting to natural gas ($A_{5,1} = 0.066$) and coal ($A_{6,1} = 0.108$), suggesting risk in green debt immediately spills into both conventional and transition-energy markets. Similarly, conventional bond innovations propagate to Brent crude ($A_{4,3} = 0.076$), highlighting the sensitivity of oil prices to bond market movements. By contrast, column 7 (EUA) is dominated by near-zero values, indicating that carbon-allowance shocks remain largely idiosyncratic at the daily horizon.

Matrix B shows the "persistence" (GARCH) effects at a longer horizon. Both green bonds ($B_{1,1} = 0.71$) and aggregate bonds ($B_{3,3} = 0.79$) exhibit the largest own memory, reflecting the slow-moving mean-reversion in volatility. Beyond these diagonals, green

bond variances also flow into ESG equities ($B_{2,1} = 0.067$) and natural gas ($B_{5,1} = 0.06$), indicating a channel through which green-bond risk elevates variance in transition-finance markets. Similarly, volatility in the aggregate-bond index spills into natural gas, Brent crude and coal, corroborating a bond-centred spillover regime. We also observe bidirectional persistence between Brent crude and global equities, indicating energy and equity market shocks reinforce one another. Many of the off-diagonal coefficients in the EUA column are both small and negative, suggesting that carbon-permit shocks tend to dampen rather than amplify volatility in other markets. Finally, variability in the broad equity index predominantly spills over into ESG equities ($B_{2,8} = 0.025$), Brent crude ($B_{4,8} = 0.081$) and carbon permits ($B_{7,8} = 0.019$), highlighting these assets as primary outlets for equity-market turbulence.

4.2 Spillover analysis

In this subsection, we quantify volatility spillovers among eight assets and address three questions: (i) which assets dominate as net senders or receivers of spillovers; (ii) the role of green assets within this connectedness network; and (iii) whether green assets behave more like other assets in their own class or more like one another, i.e., whether they share a distinct 'green factor'. Table 3 presents the spillover measures and balance indices introduced in Section 2.2. A balance index greater than unity indicates that an asset is a net sender of spillovers, whereas a value below one implies that it is a net receiver.

On the fixed-income side, both aggregate bonds (AGGB, 1.599) and green bonds (GBOND, 1.400) behave as net volatility senders, exporting roughly 60% and 40% more risk, respectively, than they absorb. This finding echoes Jovović and Popović (2025), who employ a Diebold–Yilmaz connectedness framework to demonstrate that both green and conventional bond markets transmit a substantial share of their volatility to other assets, as well as Mensi et al. (2024), who combine the Diebold and Yilmaz spillover

Table 3 – Spillover matrix, cumulative IN- and OUT-totals, and balance ratios

	GBOND	ESG	AGGB	BRENT	GAS	COAL	EUA	STOCK	**Total From**
GBOND	35.19	14.92	30.10	5.58	10.34	14.81	1.67	10.06	87.49
ESG	24.03	17.90	21.69	5.73	8.19	12.43	2.02	10.01	84.09
AGGB	26.19	10.49	29.59	5.10	9.50	14.17	1.90	8.21	75.56
BRENT	11.32	7.19	11.99	5.70	3.89	5.92	2.28	6.87	49.45
GAS	22.51	10.46	21.31	4.34	10.11	12.21	1.39	7.14	79.36
COAL	19.54	9.55	17.41	3.60	7.79	15.53	1.83	5.98	65.69
EUA	5.67	4.74	5.35	2.54	2.36	4.06	5.20	4.15	28.88
STOCK	13.23	10.32	12.99	6.40	4.23	6.30	2.98	10.33	56.46
Total To	122.48	67.67	120.84	33.29	46.29	69.91	14.07	52.41	–
Balance Index	1.400	0.805	1.599	0.673	0.583	1.064	0.487	0.928	

index and the quantile connectedness approach to show that green bonds are volatility exporters under typical market conditions.

Turning to the energy-commodity segment, both crude oil (BRENT, 0.673) and natural gas (GAS, 0.583) act as net receivers, with balance indices below unity, while coal (1.064) is a marginal net transmitter. This ranking is consistent with Asadi et al. (2022), who use a time- and frequency-domain Diebold–Yilmaz connectedness framework to show that crude oil and natural gas predominantly absorb volatility spillovers, whereas coal consistently transmits risk to other markets. However, it contrasts with the Turkey-focused study of Coskun and Taspinar (2022), where natural-gas prices act as transmitters, while coal and oil mostly absorbed shocks. This discrepancy likely reflects differences in network composition and market structure: the Turkish study investigates volatility spillovers among Turkish energy stocks, the BIST electricity index, and three fossil-fuel commodities (crude oil, natural gas, and coal), where strong gas to energy stocks ties make gas appear as a net sender and coal as a receiver.

On the equity side, both the broad market index and its ESG counterpart behave as net receivers, with balance indices just below one. This mirrors earlier evidence from Tian and Hamori (2016), who document that the S&P500 consistently absorbs, more volatility than transmits it; Mensi et al. (2023), who find that the S&P 500 is a net

receiver in the short run; and Zhang et al. (2022), who demonstrate that the broad ESG equity index absorbs substantially more volatility than they transmit when sharing a system with stronger senders such as carbon futures or commodities.

Finally, the carbon-credit market (EUA, 0.487) emerges as a pronounced net receiver, consistent with Maneejuk et al. (2025), who use a Copula-Quantile CoVaR framework to show that carbon futures mainly absorb volatility, especially downside risks from energy markets. This result is also consistent with Pakrooh and Manera (2024), who employ time-varying parameter VAR with stochastic volatility and copula-vine dependence models to demonstrate that the EU emission allowance market persistently receives volatility spillovers from energy, metal, and equity markets. By contrast, Zhang et al. (2022) find carbon-emission futures (CEF) to be the principal volatility transmitter within a green-only asset network, and Ren et al. (2024) identify the carbon market as the dominant source of informational-inefficiency spillovers across both conventional energy and green assets. The differences likely reflect sample design. Zhang et al. (2022) work with a narrower, green-only asset network where CEF is the most liquid asset and therefore leads the group. In contrast, Ren et al. (2024) analyse a shorter window (2017–2022), a period when carbon prices frequently led broader market moves.

To conclude, our baseline analysis of eight series points to a volatility regime dominated by bonds. Within the network, we identify four green-asset nodes: green bonds as net transmitters of volatility, ESG equities as net receivers, natural gas as a net receiver, and carbon credits as a net receiver.[1] No single, overarching "green-asset" pattern emerges. Instead, each green instrument behaves like its conventional counterpart. Green bonds mirror the role of aggregate bonds (both are net transmitters), ESG eq-

[1]There is emerging consensus that both natural gas and carbon credits qualify as green-transition assets. Specifically, the EU Complementary Climate Delegated Act (EU 2022/1214) designates low-emission fossil-gas power as an "environmentally sustainable transitional activity" under the EU Taxonomy (See `https://eur-lex.europa.eu/eli/reg_del/2022/1214/oj/eng`), while energy transition studies such as Gürsan and de Gooyert (2021) and Ediger and Berk (2023) describe natural gas as a bridge fuel toward full decarbonization. Similarly, empirical finance papers treat carbon credit futures as investable green instruments include Demiralay et al. (2022), Hanif et al. (2025) and Cao and Xie (2024), among others.

uities resemble traditional equities (net receivers) and natural gas aligns with oil (both net receivers) while differing from coal, which remains a net transmitter.

4.3 Impulse response analysis

Lastly, we use the MGARCH-based impulse response to show how shocks propagate to other markets during crises. We focus on four events in our sample period: i) 11 March, 2020 - when the World Health Organization (WHO) declared COVID-19 a global pandemic; ii) 14 July 2021 - when the European Commission unveiled the Fit-for-55 package, raising the 2030 emissions-reduction target and signalling tighter EU ETS caps; iii) 24 February 2022 - when Russia's invasion of Ukraine triggered EU and UK emergency energy-security measures (gas-storage mandates, LNG procurement, temporary coal-plant extensions), setting off the largest natural-gas and coal price spikes in decades; and iv) 16 August 2022 - when the U.S. Inflation Reduction Act (IRA) was signed into law, allocating $369 billion in tax credits and incentives for solar, wind, hydrogen, and grid storage, and sharply increasing expected clean-energy deployment.

Each of these shocks originates in a different market - global equities (COVID), EU carbon allowances (Fit-for-55), natural gas (Russia-Ukraine), and ESG equities (IRA) - and then propagates with varying intensity across the system.

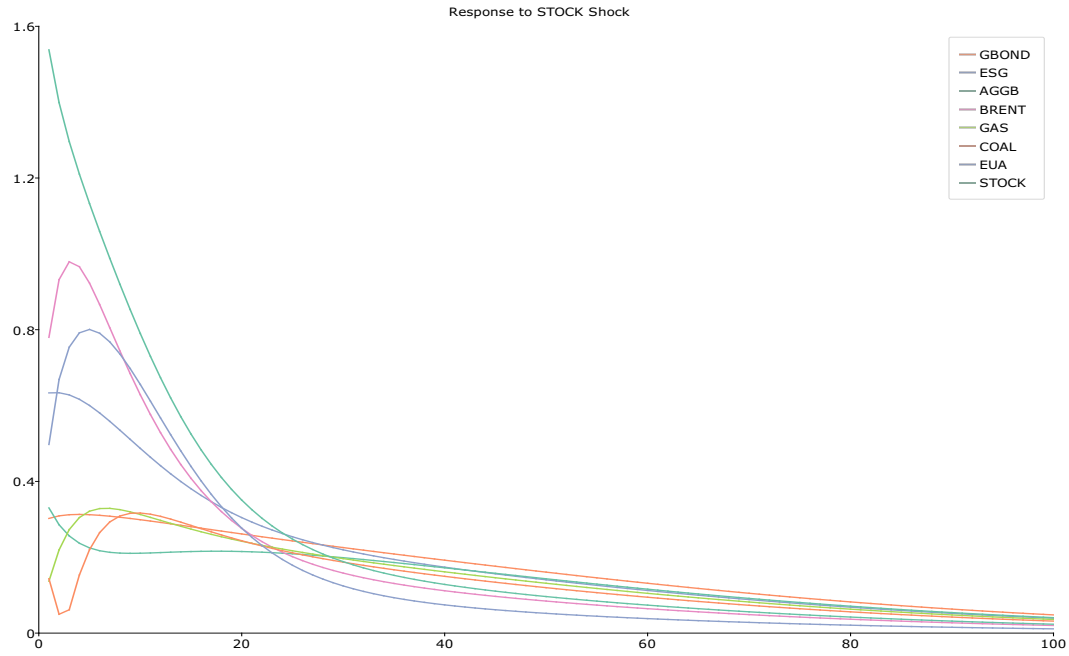


Figure 2 – Impulse Response Functions: originate market Stock - COVID19 shock

Figures 2 through 5 show the 100-day generalised impulse responses in historical sequence: COVID equity shock → EU Fit-for-55 carbon shock → Russia–Ukraine gas shock → IRA ESG equity shock. Three key insights emerge that align closely with the spillover matrices.

First, macro-equity shocks generate the widest and most persistent waves. The COVID-equity shock falls most heavily on stocks themselves, with conditional variance spiking to about 1.5 on day 1 and then waning steadily over the next 100 days. At the same time, all other markets register smaller, hump-shaped responses peaking between days 3 and 5, illustrating how equity-market volatility gradually ripples into other asset classes. Among these secondary effects, Brent crude, carbon permits and ESG equities show the largest peaks, matching the spillover magnitudes in Table 3, and serve as the main outlets for turbulence. By contrast, coal, natural gas, aggregate bonds and green bonds show the weakest reactions, peaking at only 0.25 to 0.3. This illustrates

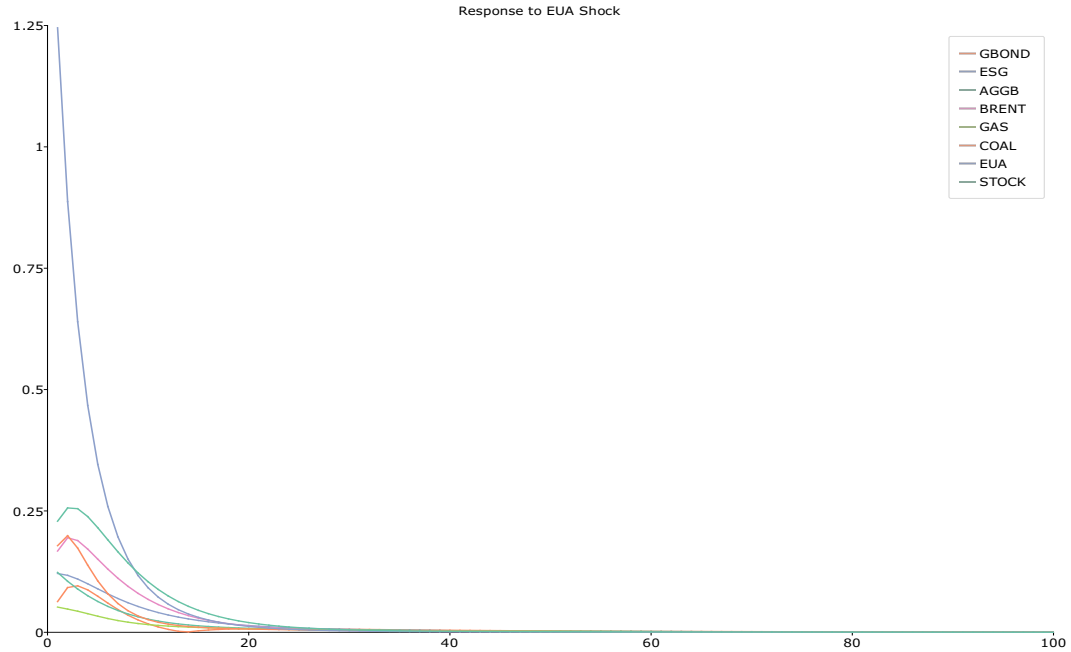


Figure 3 – Impulse Response Functions: originate market EUA - EU ETS allowances

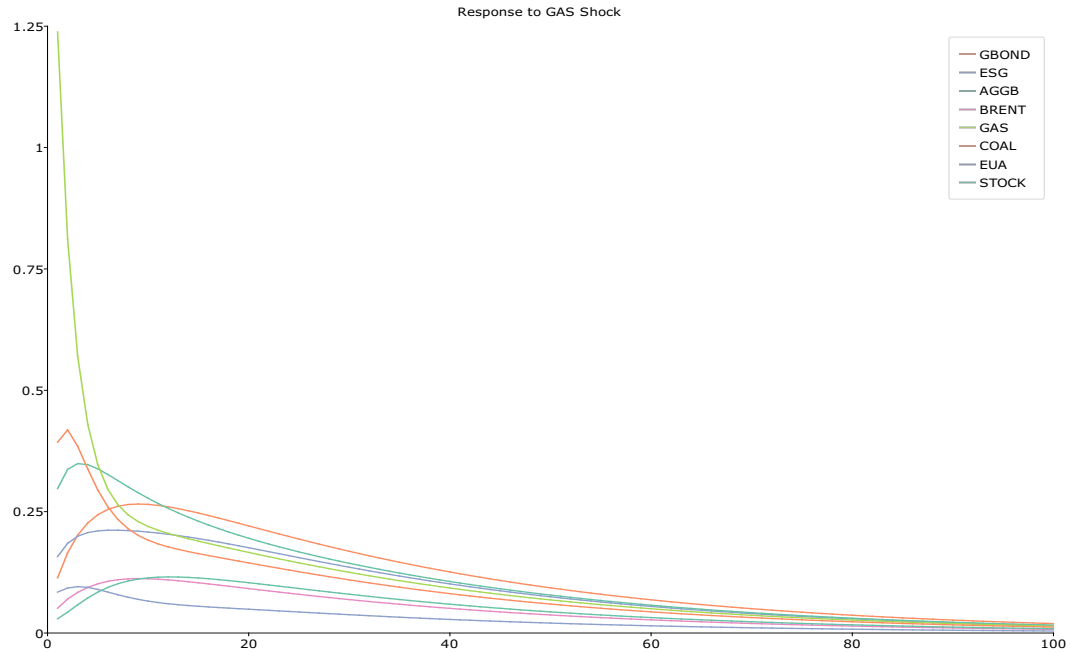


Figure 4 – Impulse Response Functions: originate market GAS - Russia–Ukraine War

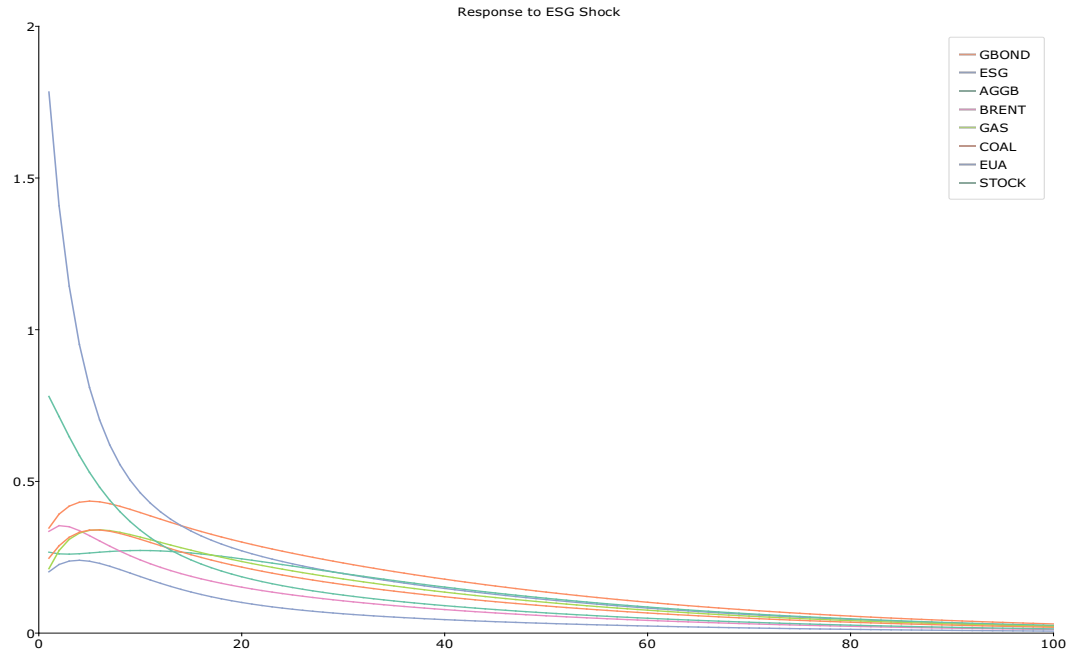


Figure 5 – Impulse Response Functions: originate market ESG - U.S. Inflation Reduction Act

the safe-haven status of bonds and the buffering effect of long-term contracts in the coal and gas markets. These dynamics echo Papadamou et al. (2021) (flight-to-quality into sovereign bonds during COVID) and Si et al. (2021) (oil produced the largest net volatility spillovers in early 2020, followed by gas, with coal least affected).

Second, policy shocks are asset-specific unless they trigger broad capital reallocation. Figure 3 reveals that the EUA shock triggered by Fit-for-55 is almost entirely self-contained, surging to about 1.25 on impact and then decaying back to zero by day 20. By contrast, all other series exhibit only tiny blips of 0.05-0.25 on day 1 and revert fully within the same 20-day window. Natural gas co-moves by only about 0.05 on impact, and even the largest spillover (to the stock index) stays below 0.3, mirroring the minimal outflows in Table 3. Together, these results confirm that carbon markets are highly idiosyncratic and that policy-driven EUA shocks remain largely insulated from the broader system. This evidence is consistent with Hanif et al. (2025) and Cao and

Xie (2024), who each show that EUA functions primarily as a receiver, transmitting only minimal volatility to other markets. By contrast, Figure 5 shows the impulse responses to an ESG equity shock triggered by the IRA first hits the ESG equity market (with an initial impact around 1.8) and then spills over into aggregate stocks, coal and other markets. Most responses follow hump-shaped patterns, peaking around 0.3–0.4 during days 3 to 5, before gradually declining and returning to zero after about 60 to 80 periods. Notably, the decay is much slower and the spillover effects are larger compared to the carbon shock. This suggests that ESG-related shocks produce more sustained and widespread effects across financial and commodity markets. These results are consistent with Bauer et al. (2023), who find that the IRA caused broad market spillovers into multiple sectors, providing clear evidence of capital reallocation triggered by climate policy. We attribute the difference between the two policy shocks to both scope and market integration: Fit-for-55 affects a compliance market with limited financial integration, while the IRA directly influences widely traded ESG equities, prompting broader capital reallocation (see Bauer et al., 2023).

Finally, Natural gas shocks are moderately persistent with selective cross-market effects. Figure 4 shows that, as expected, the gas market exhibits the strongest immediate reaction, surging to around 1.25 on impact, then decaying rapidly. Other markets respond more moderately. Green bonds, aggregate bonds and stock indices exhibit moderate hump-shaped responses, peaking within the first 5-10 days, indicating meaningful but transient spillovers from gas to financial markets. This pattern is corroborated by Ha (2023)'s continuous wavelet analysis, which shows that during the Russia-Ukraine conflict, natural gas volatility acts as a high-frequency transmitter, triggering pronounced, hump-shaped spillovers into equity and sovereign-bond markets that peak within the first week.

Overall, the impulse response analysis confirms the matrix-based interpretation. Macro-equity shocks cause fast and broad effects, carbon-policy shocks remain con-

tained, ESG shocks generate wider and more persistent effects and gas shocks fall in between, showing moderate persistence with selective spillovers during events like the Russia-Ukraine war.

4.4 Robustness checks

This subsection tests the stability of our results by replacing the broad ESG index with solar and wind equities and by comparing pre- and post-war subsamples.

Technology-specific ESG index

To test whether our previous results hinge on the use of the broad ESG equity index (ESG) in the baseline model, we re-estimate the system by replacing ESG equities with two industry-specific clean energy indices, namely the solar energy index (Solar) and the wind energy index (Wind). This substitution is motivated by two key considerations. First, the broad ESG index covers a wide range of themes, including clean energy, sustainable water, and pollution prevention. Within clean energy, solar and wind face distinct economic drivers. Solar is shaped by polysilicon prices and Chinese export policy, while wind depends on rare-earth materials and auction schemes. A broad index such as the MSCI ACWI blends these differences, masking sector-specific volatility. Disaggregating solar and wind, therefore, allows us to capture their unique risk profiles. Second, many investors adopt a core-satellite approach, combining broad ESG exposure with targeted allocations to solar or wind. If spillover results remain consistent when we replace the broad ESG index with these narrower sectors, it reinforces the relevance of our findings for actual investment behaviour.

Table 4 shows that the split alters the spillover network in two noteworthy ways. First, solar equities emerge as the single-largest net transmitter (SOLAR = 2.003), while wind remains a net receiver (WIND = 0.858), similar to the broad ESG equity index in the benchmark model (ESG = 0.805). This result is intuitive: the solar industry is highly sensitive to supply-chain disruptions (e.g., polysilicon shortages, Chinese export

Table 4 – Spillover matrix with Solar and Wind replacing the broad ESG sleeve

	GBOND	AGGB	BRENT	GAS	COAL	EUA	STOCK	SOLAR	WIND	**Tota**
GBOND	24.247	11.410	6.574	13.555	11.621	2.144	6.902	9.693	13.679	
AGGB	12.042	7.296	4.102	9.482	7.493	1.656	3.776	5.362	7.187	
BRENT	9.693	6.823	20.541	7.302	7.935	2.834	9.157	11.674	15.456	
GAS	13.470	7.068	3.455	22.111	14.727	2.020	3.543	6.293	7.053	
COAL	13.847	7.443	5.015	15.191	18.353	2.406	4.797	7.033	9.641	
EUA	4.723	3.523	3.867	3.001	2.631	7.566	4.165	5.081	8.070	
STOCK	6.308	4.256	7.570	4.514	4.684	1.437	5.954	6.763	9.029	
SOLAR	5.539	3.506	6.234	2.704	3.460	1.409	4.695	9.544	8.114	
WIND	16.124	10.746	12.100	7.797	7.329	3.204	14.309	19.520	33.242	
Total To	81.745	54.774	48.918	63.547	59.881	17.108	51.345	71.418	78.229	
Balance Index	1.082	1.072	0.690	1.103	0.916	0.488	1.152	2.003	0.858	

policy) and policy shifts (e.g., IRA credits, tariffs) since 2021, while wind equities benefit from long-term power-purchase agreements and lower input-cost volatility, dampening their spillovers. This aligns with Liu et al. (2021), Khalfaoui et al. (2022), and Guo et al. (2023), who all document solar equities acting as net transmitters under various frameworks. However, it contrasts with Coskun (2023) and Gong et al. (2023), who identify solar as a net receiver in their average-spillover and quantile-VAR analyses, respectively. The divergence likely reflects differences in sample periods and index composition. Second, natural gas flips from a strong receiver to a marginal transmitter (0.583 vs. 1.103). This shift likely reflects solar-specific volatility exposure. Once separated from the ESG index, solar becomes a strong transmitter. Because of the close linkage between solar and gas via electricity markets and energy transition dynamics, some of these shocks spill into the gas market, increasing its volatility and shifting its role in the network.

Other core patterns show relatively small shifts. Aggregate bonds and green bonds remain net transmitters, although their spillover intensity weakens (1.599 vs. 1.072 for aggregate bonds and 1.400 vs. 1.082 for green bonds). This is possibly due to volatility being redirected from bonds to solar, which now acts as a dominant transmitter after disaggregating the ESG index. Meanwhile, carbon credits and Brent crude remain almost completely unaffected, continuing to act as volatility sinks (0.487 vs. 0.488 for EUA

and 0.673 vs. 0.690 for BRENT), suggesting that their roles in the broader transition finance volatility network remain stable and largely insulated from structural changes in the clean-energy equity composition.

Subsample Analysis

To gauge how the energy-security shock altered cross-asset transmission, we reestimate the AL-MGARCH model on two non-overlapping windows: *Pre-war* (07 November 2018 – 23 February 2022, 788 observations) and *Post-war* (24 February 2022 – 19 February 2025, 721 observations). The cut–off is economically meaningful for two reasons.

First, energy policy shifted after Russia's invasion on Ukraine. The EU's REPowerEU plan shifted from speeding up decarbonization to ensuring energy security, through additional LNG cargos, the temporary extension of selected coal-fired power plants' operational lifespans, and a slowdown of ETS Phase IV reforms.[2] At the same time, the U.S. released reserves from its Strategic Petroleum Reserve to stabilize oil and gas prices. IEA data show that EU coal-fired generation rose by nearly 7% in 2022, the first increase in a decade, while utility-scale solar capital expenditures were delayed by polysilicon shortages.[3]

Second, markets signalled a regime shift. Option-implied volatility for TTF natural gas averaged 165% annually in 2022–23 versus 75% in 2017–21, while open interest in the Solactive Solar index fell 25% following the war-related supply-chain squeeze. These shifts suggest the post-war period is governed by a different volatility hierarchy, with fossil-fuel contracts regaining systemic importance and clean-energy equities behaving more like receivers than transmitters.

In the Adaptive Lasso, we select λ using the first 600 observations for estimation and the remaining 121 for forecasting. The optimal λ is then chosen, and the results are reported in Table 5.

[2]See `https://eur-lex.europa.eu/legal-content/EN/TXT/?uri=CELEX:52022DC0230`

[3]See `https://iea.blob.core.windows.net/assets/86ede39e-4436-42d7-ba2a-edf61467e070/WorldEnergyOutlook2023.pdf`

Table 5 – Spillover matrix after the Russia–Ukraine shock

	GBOND	ESG	AGGB	BRENT	GAS	COAL	EUA	STOCK	**Total From**
GBOND	12.210	17.564	17.576	14.438	41.016	37.631	5.817	6.261	140.30
ESG	4.454	9.488	2.617	4.347	4.162	6.893	1.820	11.772	36.07
AGGB	6.989	21.556	18.444	15.196	42.159	38.897	5.839	6.683	137.32
BRENT	13.509	29.869	13.368	30.699	35.469	34.449	7.121	15.873	149.66
GAS	29.086	52.132	39.750	35.217	101.591	70.500	12.065	17.703	256.45
COAL	27.510	61.387	42.012	32.338	103.198	75.215	16.212	34.211	316.87
EUA	8.590	22.418	16.859	14.093	43.907	35.594	6.695	8.402	149.86
STOCK	8.860	28.880	15.428	10.836	35.526	22.120	7.426	25.385	129.08
Total To	98.998	233.805	147.612	126.464	305.437	246.085	56.300	100.905	–
Balance	0.706	6.483	1.075	0.845	1.191	0.777	0.376	0.782	

Table 5 documents a realignment of spillover patterns following the Russia-Ukraine conflict. Aggregate spillovers ("Total To") increased most for energy commodities. Gas rose from 46.29 to 305.44, Coal from about 70 to 246.09 and Brent crude from 33.29 to 126.46, suggesting that supply-side disruptions have greatly strengthened their influence across other markets. Similarly, received spillovers ("Total From") jumped for Coal (65.69→316.87), Gas (79.36→256.45) and Brent crude (49.45→149.66), highlighting how sharp price moves reverberated within those sectors and spillover to their counterparts. These findings align with Chen et al. (2023), who show that gas market volatility became much more persistent after February 2022, with elevated levels taking longer to return to normal than before the invasion. They are also consistent with Zhang et al.'s (2024) finding that a sharp rise in high-frequency crude oil price fluctuations after the outbreak of the Russia-Ukraine war, using an EMC framework. The balance index for ESG stocks climbed from 0.81 to 6.48, reflecting their emergence as net volatility sources amid rapid portfolio reallocations. This transformation is consistent with Jiang et al. (2023), who found that ESG equities shifted from risk absorbers to risk propagators after the invasion, especially toward green bonds. It also aligns with El Khoury et al. (2023), who showed that ESG indices became more volatile and more strongly connected to other sectors during the war.

By contrast, both green bonds and the aggregate bond index saw their balance indices fall. Green bonds dropped below 1, shifting from net transmitter to net receiver, and aggregate bonds declined from 1.60 to 1.08 as investors sought safe havens, effectively ending the prewar bond-centered regime (Mensi et al., 2024). Even the carbon credit and broad equities, already net receivers before the conflict, fell further below 1, deepening their roles as shock absorbers.

Overall, the post-war period confirms the regime-dependent spillovers, with bond volatility leading when energy supplies are ample, and energy commodities, such as natural gas and Brent crude, driving volatility when supplies are threatened, while bonds and equities revert to absorbing shocks.

4.5 Policy implications

The spillover evidence from both the baseline model and the robustness checks highlights three areas where policymakers can help dampen transition-risk volatility and improve market resilience. First, stabilizing bond market requires support for both green and conventional bonds. The balance indices for both green bonds and their conventional counterparts act as net transmitters in normal regimes, with the latter amplifying macro shocks. When interest rates adjust sharply, liquidity can dry up across segments of the bond market. If central banks restrict asset-purchase or repo facilities to conventional bonds, the green-bond market may be left illiquid. To avoid this outcome, central banks should include green bonds in their programmes so trading remains liquid even under stress. This helps stabilise prices and limits spillovers into stocks and energy markets.

Second, strengthening gas supply resilience will help curb system-wide volatility. Recall that in the post-war period, when pipelines and LNG supplies tightened, natural gas became the dominant volatility transmitter. Policies that improve LNG storage or diversify pipeline supply, therefore, help dampen volatility across the financial-energy network. The results strengthen the case for EU "joint gas purchasing" and U.S. strategic

LNG reserve initiatives aimed at smoothing price spikes.

Finally, avoiding volatility concentration through diversified renewable support will enhance stability. When solar and wind are analysed separately, the solar index emerges as the main transmitter of shocks, while wind a moderate receiver. Concentrating support in a single technology, such as front-loaded solar PV credits, heightens sectoral sensitivity and amplifies spillovers. Thus, a more balanced mix across various renewable technologies would spread risks and prevent volatility from being funnelled through a single sector.

5 Conclusion

This paper develops an Adaptive–Lasso MGARCH framework that extracts a sparse, economically interpretable map of volatility spillovers from daily data alone—precisely the setting where transition-finance assets lack reliable intraday histories. By applying an L_1 penalty with adaptive weights to a MGARCH(1,1), we shrink negligible cross-market effects to zero and retain the dominant transmission channels, bringing the parameter count down from $O(N^2)$ to $O(N)$ while preserving oracle-selection properties. Recasting the model in vector-MEM form generalises Diebold–Yilmaz–style connectedness to daily returns, enabling single-step monitoring of transition-risk networks without realized volatilities.

Empirically, three results stand out. First, over the full 2017-2025 window, conventional and labelled green bonds are the largest net transmitters of volatility, while natural gas, Brent and coal mostly absorb shocks. Macro-rate uncertainty rather than commodity stress is, therefore, the primary driver of cross-asset variance in tranquil periods. Second, a post-invasion subsample (Feb 2022-Jun 2025) shows the hierarchy reversing. LNG and coal futures become the systemic hubs, radiating volatility into bonds, carbon permits and equities. This regime switch highlights how quickly transition risk

can migrate when policy priorities flip from decarbonisation to supply security. Finally, disaggregating the green-equity sleeve reveals that pure-play Solar equities are now the single biggest transmitter within the asset class, whereas Wind remains a volatility sink. Policy incentives that concentrate risk in one technology can therefore amplify, rather than diversify, transition volatility.

Taken together, these results suggest important policy priorities. Stabilising the bond complex is critical when macro shocks are rate-driven, while stabilising gas and coal markets becomes paramount in an energy-security regime. Emergency liquidity facilities should extend both conventional and green bonds, while gas-storage and joint-purchasing programmes can play a macro-prudential role by damping commodity-to-finance spillovers. Finally, subsidy design should consider volatility links between renewable technologies and avoid concentration in one sector, which could expose capital markets to higher risk.

Overall, our findings demonstrate that sparsity-based MGARCH models can extract rich transition-risk insights from relatively short daily series, providing regulators and market participants with a transparent tool for monitoring the evolving network of green-finance volatility.

References

Antonakakis, N., Chatziantoniou, I., Gabauer, D., 2020. Refined measures of dynamic connectedness based on time-varying parameter vector autoregressions. Journal of Risk and Financial Management 13, 84. doi:10.3390/jrfm13040084.

Arnold, T., Earl, J.H., Farizo, J., North, D., 2024. Endowment asset allocations: insights and strategies. Journal of Asset Management 25, 349–368.

Asadi, M., Roubaud, D., Tiwari, A.K., 2022. Volatility spillovers amid crude oil, natural gas, coal, stock, and currency markets in the us and china based on time and frequency domain connectedness. Energy Economics 109, 105961.

Audrino, F., Camponovo, L., 2013. Oracle Properties and Finite Sample Inference of

the Adaptive Lasso for Time Series Regression Models. Economics Working Paper Series 1327. University of St. Gallen, School of Economics and Political Science. St. Gallen. URL: http://ux-tauri.unisg.ch/RePEc/usg/econwp/EWP-1327.pdf. rePEc:usg:econwp:2013:27.

Bauer, M.D., Offner, E.A., Rudebusch, G.D., 2023. The effect of US climate policy on financial markets: An event study of the Inflation Reduction Act. Technical Report. CESifo Working Paper.

Bauwens, L., Laurent, S., Rombouts, J., 2006. Multivariate garch models: A survey. Journal of Applied Econometrics 21, 79–109.

Bauwens, L., Xu, Y., 2023. Dcc- and deco-heavy: Multivariate garch models based on realized variances and correlations. International Journal of Forecasting 39, 938–955.

Bauwens, L., Xu, Y., 2025. The contribution of realized variance–covariance models to the economic value of volatility timing. International Journal of Forecasting 41, 1165–1183.

Bouri, E., Rognone, L., Sokhanvar, A., Wang, Z., 2023. From climate risk to the returns and volatility of energy assets and green bonds: A predictability analysis under various conditions. Technological Forecasting and Social Change 194, 122682.

Cao, G., Xie, F., 2024. Extreme risk spillovers across energy and carbon markets: Evidence from the quantile extended joint connectedness approach. International Journal of Finance & Economics 29, 2155–2175.

Cattivelli, L., Gallo, G.M., 2019. Adaptive lasso for vector multiplicative error models. Quantitative Finance , 1–20.

Chatziantoniou, I., Abakah, E.J.A., Gabauer, D., Tiwari, A.K., 2022. Quantile time–frequency price connectedness between green bond, green equity, sustainable investments and clean energy markets. Journal of Cleaner Production 361, 132088.

Chen, S., Bouteska, A., Sharif, T., Abedin, M.Z., 2023. The russia–ukraine war and energy market volatility: A novel application of the volatility ratio in the context of natural gas. Resources Policy 85, 103792.

Conrad, C., Karanasos, M., 2010. Negative volatility spillovers in symmetric and asymmetric garch models. Econometric Reviews 29, 474–513.

Corsi, F., 2009. A simple approximate long-memory model of realized volatility. Journal of Financial Econometrics 7, 174–196.

Coskun, M., 2023. Dynamic correlations and volatility spillovers between subsectoral clean-energy stocks and commodity futures markets: A hedging perspective. Journal of Futures Markets 43, 1727–1749.

Coskun, M., Taspinar, N., 2022. Volatility spillovers between turkish energy stocks and fossil fuel energy commodities based on time and frequency domain approaches. Resources Policy 79, 102968.

Demiralay, S., Gencer, H.G., Bayraci, S., 2022. Carbon credit futures as an emerging asset: Hedging, diversification and downside risks. Energy Economics 113, 106196.

Diebold, F.X., Yilmaz, K., 2012. Better to give than to receive: Forecast-based measurement of connectedness. International Journal of Forecasting 28, 57–66.

Diebold, F.X., Yilmaz, K., 2014. On the network topology of variance decompositions: Measuring the connectedness of financial firms. Journal of Econometrics 182, 119–134.

Díaz, A., Livingston, M., 2025. On-the-run liquidity phenomenon in the u.s. treasury bond market: A tvp-var analysis. Working Paper .

Ediger, V.Ş., Berk, I., 2023. Future availability of natural gas: Can it support sustainable energy transition? Resources Policy 85, 103824.

El Khoury, R., Nasrallah, N., Hussainey, K., Assaf, R., 2023. Spillover analysis across fintech, esg, and renewable energy indices before and during the russia–ukraine war: International evidence. Journal of International Financial Management & Accounting 34, 279–317.

Engle, R., Gallo, G., Velucchi, M., 2012. Volatility spillovers in east asian financial markets: A mem-based approach. The Review of Economics and Statistics 94, 222–223.

Engle, R.F., Kroner, K.F., 1995. Multivariate simultaneous garch. Econometric Theory 11, 122–150.

Estrada, J., 2023. Multifactor funds: an early (bearish) assessment. Journal of Asset Management , 1.

Ewing, B.T., Payne, J.E., 2003. Volatility spillovers between sectors of the dow jones industrial average. Economics Letters 79, 475–479.

Fields, M., Lindequist, D., 2024. Global spillovers of us climate policy risk: Evidence from eu carbon emissions futures. Energy Economics 139, 107931.

Gabauer, D., Gupta, R., 2018. On the transmission mechanism of country-specific and international economic uncertainty spillovers: Evidence from a tvp-var connectedness decomposition approach. Economics Letters 171, 63–71.

Gong, X.L., Zhao, M., Wu, Z.C., Jia, K.W., Xiong, X., 2023. Research on tail risk contagion in international energy markets—the quantile time-frequency volatility spillover perspective. Energy Economics 121, 106678.

Guo, X., Wang, Y., Hao, Y., Zhang, W., 2023. Spillover effect among carbon bond market, carbon stock market and energy stock market: Evidence from china. Finance Research Letters 58, 104521.

Gurrib, I., Nourani, M., Bhaskaran, R.K., 2022. Energy crypto currencies and leading us energy stock prices: are fibonacci retracements profitable? Financial Innovation 8, 8.

Gürsan, C., de Gooyert, V., 2021. The systemic impact of a transition fuel: Does natural gas help or hinder the energy transition? Renewable and Sustainable Energy Reviews 138, 110552.

Ha, L.T., 2023. Dynamic connectedness between green energy and carbon risk during russia-ukraine conflict: new evidence from a wavelet analysis. Environmental Science and Pollution Research 30, 79297–79314.

Hachicha, N., Amar, A.B., Slimane, I.B., Bellalah, M., Prigent, J.L., 2022. Dynamic connectedness and optimal hedging strategy among commodities and financial indices. International Review of Financial Analysis 83, 102290.

Hamao, Y., Masulis, R.W., Ng, V., 1990. Correlations in price changes and volatility across international stock markets. Review of Financial Studies 3, 281–307.

Hanif, W., El Khoury, R., Gubareva, M., Teplova, T., 2025. Asymmetric connectedness among regional green economies, carbon markets, and oil shocks. International Review of Economics & Finance , 104416.

Hassan, M.K., Hasan, M.B., Halim, Z.A., Maroney, N., Rashid, M.M., 2022. Exploring the dynamic spillover of cryptocurrency environmental attention across the commodities, green bonds, and environment-related stocks. The North American Journal of Economics and Finance 61, 101700.

Ito, K., Yoshiba, T., 2025. Dynamic asymmetric tail dependence structure among multi-asset classes for portfolio management: Dynamic skew-t copula approach. International Review of Economics & Finance 97, 103724.

Jiang, W., Dong, L., Chen, Y., 2023. Time-frequency connectedness among traditional/new energy, green finance, and esg in pre-and post-russia-ukraine war periods. Resources Policy 83, 103618.

Jovović, J., Popović, S., 2025. Investigating volatility spillovers: Connectedness between green bonds, conventional bonds, and energy markets. Research in International Business and Finance 76, 102850.

Kacperczyk, M., Nosal, J., Wang, T., 2025. Global volatility and firm-level capital flows. Journal of Financial Economics 169, 104078.

Kang, S.H., Maitra, D., Dash, S.R., Brooks, R., 2019. Dynamic spillovers and connectedness between stock, commodities, bonds, and vix markets. Pacific-Basin Finance Journal 58, 101221.

Khalfaoui, R., Jabeur, S.B., Dogan, B., 2022. The spillover effects and connectedness among green commodities, bitcoins, and us stock markets: Evidence from the quantile var network. Journal of environmental management 306, 114493.

Koutmos, G., 1999. Return and volatility spillovers among major stock markets. Journal of International Money and Finance 18, 687–700.

Leone, M., Manelli, A., Pace, R., 2025. Energy, metals, cereals and g7 indices: Russia-ukraine conflict and risk spillovers. Finance Research Letters , 107557.

Liu, M., 2022. The driving forces of green bond market volatility and the response of the market to the covid-19 pandemic. Economic Analysis and Policy 75, 288–309.

Liu, N., Liu, C., Da, B., Zhang, T., Guan, F., 2021. Dependence and risk spillovers between green bonds and clean energy markets. Journal of Cleaner Production 279, 123595.

Liu, Z., Wang, Y., Yuan, X., Ding, Z., Ji, Q., 2025. Geopolitical risk and vulnerability of energy markets. Energy Economics 141, 108055.

Lucey, B., Ren, B., 2023. Time-varying tail risk connectedness among sustainability-related products and fossil energy investments. Energy Economics 126, 106812.

Maneejuk, P., Huang, W., Yamaka, W., 2025. Asymmetric volatility spillover effects from energy, agriculture, green bond, and financial market uncertainty on carbon market during major market crisis. Energy Economics 145, 108430.

Mensi, W., Al-Yahyaee, K.H., Vo, X.V., Kang, S.H., 2021. Dynamic spillover and connectedness between oil futures and european bonds. The North American Journal of Economics and Finance 56, 101342.

Mensi, W., Aslan, A., Vo, X.V., Kang, S.H., 2023. Time-frequency spillovers and connectedness between precious metals, oil futures and financial markets: Hedge and safe haven implications. International Review of Economics & Finance 83, 219–232.

Mensi, W., Selmi, R., Al-Kharusi, S., Belghouthi, H.E., Kang, S.H., 2024. Connectedness between green bonds, conventional bonds, oil, heating oil, natural gas, and petrol: new evidence during bear and bull market scenarios. Resources Policy 91, 104888.

Pakrooh, P., Manera, M., 2024. Causality, connectedness, and volatility pass-through among energy-metal-stock-carbon markets: new evidence from the eu. Resources Policy 99, 105408.

Papadamou, S., Fassas, A.P., Kenourgios, D., Dimitriou, D., 2021. Flight-to-quality between global stock and bond markets in the covid era. Finance Research Letters 38, 101852.

Reboredo, J.C., 2018. Green bond and financial markets: Co-movement, diversification and price spillover effects. Energy Economics 74, 38–50.

Reboredo, J.C., Ugolini, A., Aiube, F.A.L., 2020. Network connectedness of green bonds and asset classes. Energy Economics 86, 104629.

Ren, X., Xiao, Y., Duan, K., Urquhart, A., 2024. Spillover effects between fossil energy and green markets: Evidence from informational inefficiency. Energy Economics 131, 107317.

Saeed, T., Bouri, E., Alsulami, H., 2021. Extreme return connectedness and its determinants between clean/green and dirty energy investments. Energy Economics 96, 105017.

Sánchez García, J., Cruz Rambaud, S., 2023. Volatility spillovers between oil and financial markets during economic and financial crises: A dynamic approach. Journal of Economics and Finance 47, 1018–1040.

Scherer, K., Scherer, B., 2025. Esg/climate vs conventional indices: Their difference in climate premium. Finance Research Letters , 107436.

Si, D.K., Li, X.L., Xu, X., Fang, Y., 2021. The risk spillover effect of the covid-19 pandemic on energy sector: Evidence from china. Energy economics 102, 105498.

Tian, S., Hamori, S., 2016. Time-varying price shock transmission and volatility spillover in foreign exchange, bond, equity, and commodity markets: Evidence from the united states. The North American Journal of Economics and Finance 38, 163–171.

Tiwari, A.K., Abakah, E.J.A., Gabauer, D., Dwumfour, R.A., 2022. Dynamic spillover effects among green bond, renewable energy stocks and carbon markets during covid-19 pandemic: Implications for hedging and investments strategies. Global Finance Journal 51, 100692.

Tiwari, A.K., Abakah, E.J.A., Shao, X., Le, T.L., Gyamfi, M.N., 2023. Financial technology stocks, green financial assets, and energy markets: A quantile causality and dependence analysis. Energy Economics 118, 106498.

Vo, D.H., 2023. Volatility spillovers across sectors and their magnitude: A sector-based analysis for australia. PLOS ONE 18, e0286528.

Wang, L., Urga, G., 2025. Optimal n-state endogenous markov-switching model for currency liquidity timing. Journal of Economic Dynamics and Control , 105137.

Wang, Y., Chang, L., 2023. Green bonds' liquidity in covid-19 and low carbon investments in china: A stochastic trend analysis. Environmental Science and Pollution Research 30, 36838–36850.

Wei, P., Yuan, K., Ren, X., Yan, C., Lu, Z., 2023. Time-varying spillover networks of green bond and related financial markets. International Review of Economics & Finance 88, 298–317.

Xu, Y., Guan, B., Lu, W., Heravi, S., 2024. Macroeconomic shocks and volatility spillovers between stock, bond, gold and crude oil markets. Energy Economics 136, 108046.

Xu, Y., Taylor, N., Lu, W., 2018. Illiquidity and volatility spillover effects in equity markets during and after the global financial crisis: An mem approach. International Review of Financial Analysis 56, 208–220.

Yao, Y., Huang, X., Li, J., 2024. l_1 regularisation for high-dimensional multivariate garch models. Risks 12, 34.

Zeng, H., Abedin, M.Z., Ahmed, A.D., Huang, Q., 2025. Extreme risk connection among the european tourism, energy and carbon emission markets. Research in International Business and Finance 74, 102693.

Zhang, Q., Hu, Y., Jiao, J., Wang, S., 2024. The impact of russia–ukraine war on crude oil prices: an emc framework. Humanities and Social Sciences Communications 11, 1–12.

Zhang, W., He, X., Hamori, S., 2022. Volatility spillover and investment strategies among sustainability-related financial indexes: Evidence from the dcc-garch-based dynamic connectedness and dcc-garch t-copula approach. International Review of Financial Analysis 83, 102223.

Zou, H., 2006. The adaptive lasso and its oracle properties. Journal of the American Statistical Association 101, 1418–1429.

Appendix A: Optimal Shrinkage Parameter and Estimation

The Adaptive-Lasso MGARCH estimator is obtained in three sequential steps.

1. **Initial QML Estimation.** Estimate an unpenalized MGARCH(1,1) model on the full sample and collect the parameter estimates $\tilde{\boldsymbol{\theta}} = (\tilde{\boldsymbol{\omega}}, \tilde{\mathbf{A}}, \tilde{\mathbf{B}})$ (see Appendix B for QML Estiamtion). Adaptive weights are then defined as

$$w_j = 1/\max\{|\tilde{\theta}_j|, \epsilon_w\}, \qquad \epsilon_w = 0.005,$$

following Audrino and Camponovo (2013) and Cattivelli and Gallo (2019).

2. **Selection of the Shrinkage Parameter $\hat{\lambda}$.** Using only the first $2T/3$ observations, solve the penalized problem (3) over a grid of $n_\lambda = 30$ equally spaced values $\{\lambda_k\}_{k=1}^{n_\lambda} \subset [\lambda_{\max}/n_\lambda, \lambda_{\max}]$, where

$$\lambda_{\max} = \frac{|\ell_T(\tilde{\boldsymbol{\theta}})|}{Tdv}, \quad d = 2N^2 + N,\ v = 10.$$

For each λ_k, produce one-step-ahead forecasts on the hold-out sample (the last $T/3$ observations) and compute the QLIK loss (Bauwens and Xu, 2023):

$$\text{QLIK}_k = \sum_{t=T-T/3+1}^{T} \left\{ \text{tr}\left[(\hat{\mathbf{H}}_{t|t-1}^{(k)})^{-1} \mathbf{H}_t \right] + \log |\hat{\mathbf{H}}_{t|t-1}^{(k)}| \right\}. \tag{12}$$

Choose $\hat{\lambda} = \arg\min_k \text{QLIK}_k$.[4]

3. **Adaptive-Lasso Estimation.** Re-estimate (3) on the full sample with $\lambda = \hat{\lambda}$, yielding the final estimator $\hat{\boldsymbol{\theta}}_{\hat{\lambda}}$.

The choice of $\lambda_{\max}$ ensures that the penalty term $\lambda \sum_j w_j |\theta_j|$—which is of order λd—is commensurate with the scaled likelihood $\ell_T(\boldsymbol{\theta})/T$. This guarantees a well-behaved U-shaped loss curve, as documented by Cattivelli and Gallo (2019).

Under regularity conditions (strict stationarity and finite fourth moments) and a penalty sequence satisfying $\lambda\sqrt{T} \to 0$ and $\lambda T \to \infty$, the Adaptive Lasso estimator enjoys the following properties:

1. *Selection consistency*: $\Pr\{\widehat{\theta}_j = 0 \Leftrightarrow \theta_{0,j} = 0\} \to 1$,
2. *Asymptotic normality*: $\sqrt{T}(\widehat{\boldsymbol{\theta}}j - \boldsymbol{\theta}_{0,j}) \xrightarrow{d} N(\mathbf{0}, \mathbf{I}^{-1})$,

matching the oracle results in Zou (2006). These results parallel (and strengthen) the sparsity and consistency properties proved for the uniform-Lasso BEKK estimator in Yao et al. (2024).

Appendix B: QML Estimation for an Unpenalized MGARCH Model

We assume that $\mathbf{e}t$ follows a multivariate normal distribution conditional on the information set $It-1$, i.e., $\mathbf{e}t|It-1 \sim N(\mathbf{0}, \mathbf{P})$. Let $\boldsymbol{\theta}' = [\boldsymbol{\theta}1', \boldsymbol{\theta}2']$, where $\boldsymbol{\theta}1' = \text{vech}(\mathbf{P})$.

[4] Alternative criteria, such as BIC or an economic-loss measure, are also admissible; see Bauwens and Xu (2025).

The operator vech stacks the lower triangular elements (excluding the diagonal) of a symmetric $(N \times N)$ matrix into a vector of length $N(N-1)/2$, and $\boldsymbol{\theta}2'$ contains the parameters governing $\boldsymbol{\varepsilon}_t$.

The log-likelihood function is given by:

$$l(\boldsymbol{\theta}) = \sum_{t=1}^{T} \ln f(\boldsymbol{\varepsilon}_t|\boldsymbol{\theta}),$$

where

$$\begin{aligned} \ln f(\boldsymbol{\varepsilon}_t|\boldsymbol{\theta}) &= -\frac{N}{2}\ln(2\pi) - \frac{1}{2}\ln|\mathbf{D}_t\mathbf{P}\mathbf{D}_t| - \frac{1}{2}\varepsilon_t'\left(\mathbf{D}_t\mathbf{P}\mathbf{D}_t\right)^{-1}\boldsymbol{\varepsilon}_t \\ &= -\frac{N}{2}\ln(2\pi) - \frac{1}{2}\ln|\mathbf{D}_t| - \frac{1}{2}\ln|\mathbf{P}| - \frac{1}{2}\boldsymbol{\varepsilon}_t' D_t^{-1} P^{-1} D_t^{-1}\boldsymbol{\varepsilon}_t \\ &= -\frac{N}{2}\ln(2\pi) - \frac{1}{2}\ln|\mathbf{D}_t| - \frac{1}{2}\ln|\mathbf{P}| - \frac{1}{2}\mathbf{e}_t'\mathbf{P}^{-1}\mathbf{e}_t \end{aligned} \tag{13}$$

where $\mathbf{D}_t = diag(\sqrt{h_{1t}}, \sqrt{h_{2t}}, ..., \sqrt{h_{Nt}})$.

If the DCC specification is employed for the conditional correlation, the correlation matrix $\mathbf{P}$ can be replaced by the identity matrix in this stage estimation. The log-likelihood function at time t is then

$$\ln f(\boldsymbol{\varepsilon}_t|\boldsymbol{\theta}_1) = -\frac{k}{2}\ln(2\pi) - \frac{1}{2}\ln|\mathbf{D}_t| - \frac{1}{2}\mathbf{e}_t'\mathbf{e}_t. \tag{14}$$

In the second stage, the dynamic correlation matrix $\mathbf{P}_t$ can be estimated using $\widehat{\mathbf{e}}_t$, where $\widehat{\mathbf{e}}_t = \boldsymbol{\varepsilon}_t \odot \widehat{\mathbf{h}}_t^{-1/2}$ and $\widehat{\mathbf{h}}_t$ is the estimated conditional variance evaluated at $\boldsymbol{\theta}_1 = \widehat{\boldsymbol{\theta}}_1$, which is obtained from the first stage estimation.

The QML estimator of the unpenalized parameter vector $\tilde{\boldsymbol{\theta}}$ is obtained by minimizing the negative log-likelihood:

$$\tilde{\boldsymbol{\theta}} = \underset{\boldsymbol{\theta}}{\operatorname{argmin}} -l(\boldsymbol{\theta}), \tag{15}$$